Single-frequency distributed Bragg reflector Tm:YAG ceramic derived all-glass fiber laser at 1.95 μm

Guo-Quan Qian(钱国权)[1], Min-Bo Wu(吴敏波)[2], Guo-Wu Tang(唐国武)[2,3,†], Min Sun(孙敏)[2,‡], Dong-Dan Chen(陈东丹)[2], Zhi-Bin Zhang(张志斌)[4], Hui Luo(罗辉)[4], and Qi Qian(钱奇)[2]

[1] *Yunnan Police College, Kunming* 650223, *China*
[2] *Guangdong Provincial Key Laboratory of Fiber Laser Materials and Applied Techniques, South China University of Technology, Guangzhou* 510640, *China*
[3] *School of Physics and Optoelectronic Engineering, Guangdong University of Technology, Guangzhou* 510006, *China*
[4] *Southwest Institute of Technical Physics, Chengdu* 610041, *China*

(Received 8 July 2022; revised manuscript received 4 September 2022; accepted manuscript online 8 September 2022)

A 135 mW single-frequency distributed Bragg reflector fiber laser at 1.95 μm was obtained based on a Tm:YAG ceramic-derived all-glass fiber. The fiber laser achieved an optical signal-to-noise ratio of ∼ 77 dB. Moreover, the threshold and linewidth of the single-frequency laser were measured to be 15.4 mW and 4.5 kHz, respectively. In addition, the measured relative intensity noise was less than −140 dB·Hz^{-1} at frequencies of over 10 MHz. The results show that the as-drawn Tm:YAG ceramic-derived all-glass fiber is highly promising for ∼ 2 μm single-frequency fiber laser applications.

Keywords: all-glass fiber, single-frequency, 2 μm fiber laser, Tm:YAG ceramic derived

PACS: 42.55.–f, 42.55.Wd **DOI:** 10.1088/1674-1056/ac904c

1. Introduction

Single-frequency fiber lasers operating at ∼ 2 μm have attracted intense attention for their wide-ranging applications, from high-resolution spectroscopy and noninvasive medicine to coherent beam combining, due to their outstanding properties of low noise, narrow linewidth and at an eye-safe wavelength regime.[1–4] Up to now, ∼ 2 μm single-frequency fiber lasers have been achieved in various cavity structures, including ring cavities, distributed feedback (DFB) cavities and distributed Bragg reflector (DBR) cavities.[5–7] More recently, Walasik *et al.* reported a 2 μm single-frequency all-fiber DFB laser source employing fiber Bragg gratings (FBGs) which has a laser linewidth of 5 kHz.[8] Here, we focus on a ∼ 2 μm single-frequency fiber laser with a DBR cavity structure. A key factor in obtaining a DBR single-frequency fiber laser is the use of high-gain glass fibers for shorting the laser cavity.[9] It is known that a high rare earth (RE) ion doping concentration can achieve a large pump absorption and high gain per unit length in the resulting glass fiber, which allows efficient laser output in a short piece of RE ion-doped active fiber.[10,11]

To date, single-frequency DBR fiber lasers at ∼ 2 μm have been developed by using different Tm^{3+}-doped glass fibers, such as silica, silicate and germanate glass fibers.[7,12,13] However, pure silica glass fibers have a low RE ion doping concentration because of the well-defined glass structure consisting of a [SiO_4] tetrahedron, which limits the gain of the resulting silica glass fibers.[14] In 2015, Fu *et al.* demonstrated a 2 μm single-frequency DBR fiber laser based on a 1.9-cm long commercially available Tm^{3+}-doped silica glass fiber; this had a maximum output power of 18 mW and a slope efficiency of 13.4% with respect to the absorbed pump of a 793 nm laser diode (LD).[7] The output power of a 2 μm single-frequency DBR fiber laser can be improved by means of in-band pumping at the 1.5 μm band.[15] Note that multicomponent glasses, which have high RE ion solubility, are usually used to fabricate high-gain glass fibers.[1,16] Geng *et al.* reported a single-frequency DBR fiber laser at 1893 nm based on a 2 cm long heavily Tm^{3+}-doped germanate glass fiber; this had a pump threshold of 30 mW and a maximum output power of 50 mW.[17] They went on to demonstrate a narrow-linewidth single-frequency DBR fiber laser at 1.95 μm with a 2 cm long heavily Tm^{3+}-doped silicate glass fiber.[12] However, the large splicing losses (∼ 2.2 dB) between the active fiber and two FBGs resulted in a relatively high threshold.[12,15] In 2018, Tang *et al.* fabricated a heavily Tm^{3+}-doped barium gallo-germanate glass fiber that had a gain per unit length of 3.6 dB·cm^{-1} at 1.95 μm.[13] A single-frequency DBR fiber laser of over 220 mW at 1.95 μm was realized in a 1.5 cm long active fiber, showing a slope efficiency of 30.2% with respect to the absorbed pump of a 1568 nm fiber laser.[13] Although the multicomponent glass fibers used in these reports possess higher RE ion solubility over the silica fiber, which enables ∼ 2 μm single-frequency DBR fiber laser operation with higher output power and slope efficiency, there are still some obstacles to their application in the aforementioned areas.[15,18] For example, their softening temperature and thermal expansion coefficient are different from those of

†Corresponding author. E-mail: guowutang@126.com
‡Corresponding author. E-mail: s452936140@163.com

© 2022 Chinese Physical Society and IOP Publishing Ltd

commercial silica glass fiber, implying that it is more challenging to achieve low-loss spliced with silica-based fiber devices, such as wavelength division multiplexer (WDM) and FBG.[7] Moreover, the resulting splice joint exhibits reduced mechanical strength, which sacrifices the reliability of the fiber laser system.[15] Therefore, the development of novel fiber materials, fiber design and fabrication techniques could facilitate some high RE ion-doped silica-based fibers becoming competitive candidates for single-frequency fiber lasers.

In recent years, RE ion-doped $Y_3Al_5O_{12}$ (YAG) single crystal or polycrystalline ceramic (precursor phase) derived all-glass fibers with novel properties have been developed and fabricated for high-power fiber lasers, ultrafast fiber lasers and single-frequency fiber lasers.[19–22] Compared with RE ion-doped silica glass fibers, YAG-derived all-glass fibers with a high yttrium (Y) and aluminum (Al) concentration in the fiber core [yttrium aluminosilicate (YAS) glass] have a higher thermal conductivity and a higher stimulated Brillouin scattering threshold, properties which are beneficial for achieving high-power single-frequency fiber lasers.[23–26] Additionally, in contrast to RE ion-doped multicomponent glass fiber, the thermal expansion coefficient and refractive index of these YAG-derived all-glass fibers better matches with the silica glass cladding, making them easier to splice with silica fibers.[22,27,28] In 2019, Zhang *et al.* demonstrated a single-frequency DBR fiber laser at 1.064 μm based on a 1.7 cm long Yb:YAG ceramic-derived all-glass fiber.[19] Although the output power and slope efficiency of the laser were relatively low, this work was the first to provide a prospect for the development of all-fiber single-frequency DBR fiber lasers by using YAG-derived all-glass fibers. Then, Liu *et al.* reported a 110 mW single-frequency DBR fiber laser at 1.064 μm with a slope efficiency of 18.5% based on a 1.4 cm long Yb:YAG crystal-derived all-glass fiber by reducing the resonance loss.[20] More recently, Xie *et al.* reported a 24.2 mW pulsed single-frequency laser at 1.55 μm based on a 1.8 cm long Er:YAG crystal-derived all-glass fiber.[29] However, single-frequency DBR fiber lasers at ∼ 2 μm based on Tm:YAG crystal or ceramic-derived all-glass fibers have never been reported.

Here, Tm:YAG ceramic-derived all-glass fiber was drawn by using the molten core method. It has a gain per unit length of 2.7 dB·cm^{-1} at 1.95 μm. The as-drawn fiber has a YAS glass core, which is composed of 14.2 mol.% Al_2O_3, 77.1 mol.% SiO_2, 6.5 mol.% Y_2O_3, and 2.25 mol.% Tm_2O_3. Details of the as-drawn YAS glass fiber can be found in Table 1. A 1.95 μm single-frequency DBR fiber laser was achieved by using a 2 cm long Tm:YAG ceramic-derived all-glass fiber. The fiber laser has a high optical signal-to-noise ratio (OSNR) of ∼ 77 dB and a low pump threshold of ∼ 15.4 mW. The direct output power of the laser reached 135 mW with a pump power of 1340 mW, corresponding to a slope efficiency of 10.2% with respect to the absorbed pump power. In addition, the linewidth and relative intensity noise (RIN) were measured. This work is a proof-of-concept that Tm:YAG-derived all-glass fiber with a high gain per unit length can be used in a compact 2 μm single-frequency DBR fiber laser.

Table 1. Properties of Tm:YAG ceramic-derived all-glass fiber.

Fiber properties	Value
Tm_2O_3 doping concentration	2.25 mol.%
Core/clad diameter	10/125 μm
Propagation loss	4.8 dB/m@1310 nm
Gain per unit length	2.7 dB/cm@1.95 μm
Splicing loss with silica fiber	0.18 dB

2. Experimental details

Tm:YAG ceramic samples were prepared by the solid-state reaction method. Commercial powders (Al_2O_3, Y_2O_3, Tm_2O_3) were weighed and then mixed. Boric acid (1 wt%) was used as a sintering aid in the samples. Column-shaped YAG ceramic samples were prepared after the pressed green bodies were sintered at 1600 °C for 5 h in a muffle furnace, and then ground and polished into cylindrical rods with a diameter of ∼ 2.8 mm. The YAG rods were washed repeatedly with dilute hydrochloric acid, alcohol and distilled water to remove the contaminated surface layer and then placed into a vacuum drying oven at 400 °C for 12 h. After preparation the initial precursor material was inserted into cylindrical silica glass tubes (optical quality 99.99%, inner diameter ∼ 3 mm, external diameter ∼ 30 mm, length ∼ 150 mm). One end of the tube was sealed using an oxyhydrogen flame. Optical fiber was prepared using a standard fiber drawing tower at a temperature of ∼ 2000 °C. During the drawing process of the molten core method, the glass cladding is similar to 'the crucible', which provides a high-temperature, high-pressure environment for the core material, and the molten core is rapidly quenched. Glass fibers with different diameters can be obtained by controlling the feeding speed, the temperature and the pulling speed. Hundreds of meters of fibers with an outer diameter of ∼ 125 μm were collected for test characterization and laser experiments.

Figure 1(a) shows the XRD pattern of the Tm:YAG ceramic sample. The diffraction peaks of the sample match well with the standard card of YAG (PDF#33-0044), suggesting that the prepared ceramic sample is pure YAG phase. Figure 1(b) shows the Raman spectra of the resulting Tm:YAS fiber core and silica glass cladding. The broad Raman bands in the fiber core and cladding indicate the amorphous state of the obtained fiber.

Figure 2(a) shows the electron micrograph image of the Tm:YAS all-glass fiber. It can be observed that the fiber core

has a good circularity. Figures 2(b)–2(e) show the electron probe microanalyzer mapping of Si, Y Al, and Tm. The Al, Tm, and Y are mainly distributed in the core region, while the Si is distributed in both the cladding and the core. In our previous work this type of YAS glass fiber was proven to be a graded refractive index fiber due to the elemental migration between the melting core and the softened cladding.[27]

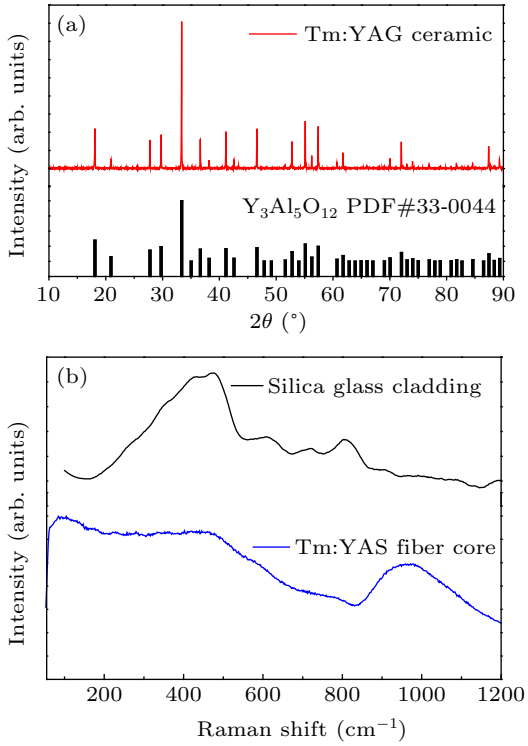


Fig. 1. (a) XRD pattern of the Tm:YAG ceramic sample. (b) Raman spectra of the resulting Tm:YAS glass fiber core and the silica glass cladding.

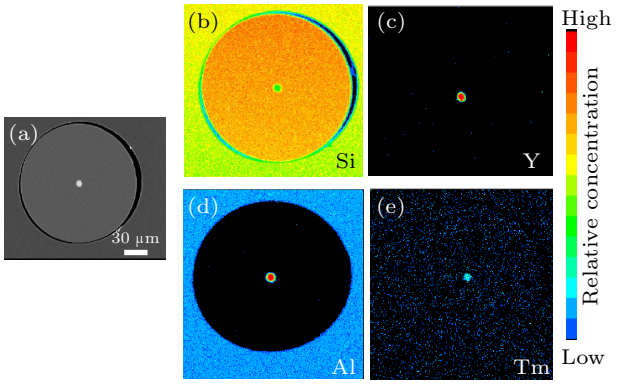


Fig. 2. (a) Electron micrograph image of the Tm:YAS all-glass fiber. (b)–(e) Electron probe microanalyzer images of the distribution of different elements across the fiber cross section.

The scheme of the experimental setup for the 1.95 μm single-frequency DBR fiber laser is shown in Fig. 3. The laser cavity combines a partial-reflection fiber Bragg grating (PR-FBG), a high-reflection fiber Bragg grating (HR-FBG) and a short piece of as-drawn gain fiber. The two ends of the gain fiber were spliced with the PR-FBG and HR-FBG. The PR-FBG has a reflectivity of 50.0% at 1950 nm and a 3 dB bandwidth of 0.09 nm. The HR-FBG has a reflectivity of 99.5% at 1950 nm. A backward pumping scheme was used in the laser experiment. The fiber laser was counter-pumped by a high-power 1610 nm fiber laser, through a 1610/1950 nm WDM. The whole laser cavity was placed in an aluminum tube, which was temperature-controlled by a cooling system with an accuracy of ±0.1 °C. To achieve efficient single-frequency laser operation, a short cavity length is necessary to enlarge the longitudinal mode spacing. For this purpose, a section of 2 cm long Tm:YAG-derived all-glass fiber was chosen as the gain fiber by the cut-back method. The laser output spectrum was monitored by an optical spectrum analyzer (AQ6375, Yokogawa, Japan) with a wavelength resolution of 0.02 nm. The single-frequency operation of the laser was confirmed by using a scanning fiber Fabry–Perot interferometer (FFPI; SA200-18B, Thorlabs) with a free-spectral range (FSR) of 1.5 GHz and a resolution of 7.5 MHz. The laser linewidth was measured by a self-heterodyne method. The RIN of the fiber laser was measured by an electrical spectrum analyzer, whose resolution bandwidth was set to 1 kHz. During each measurement of RIN the laser power was attenuated to 0.5 mW before being injected into a photoelectric detector.

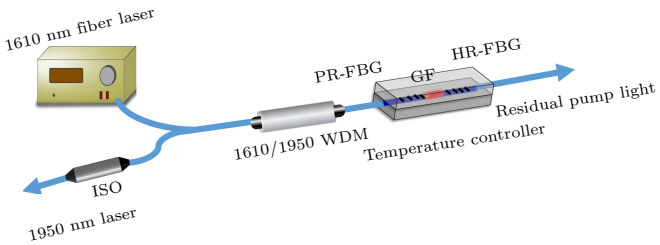


Fig. 3. Scheme of the experimental setup for the 1.95 μm single-frequency DBR fiber laser based on the as-drawn gain fiber (GF).

3. Results and discussion

The laser output spectrum is shown in Fig. 4(a). The achieved laser has a central wavelength of 1950 nm with an OSNR of ∼ 77 dB. The laser output power and the residual power were measured by a standard power meter. Figure 4(b) shows the laser output power as a function of the absorbed pump power. The laser threshold was measured to be ∼ 15.4 mW. The fiber laser yields a maximum laser output power of 135 mW with a slope efficiency of 10.2%. Note that the phenomenon of power saturation was not observed, suggesting that the output power could be further improved by using a higher available pump power. The stability of the laser output power at 60 mW was measured for 40 min; the result is shown in the inset of Fig. 4(b). The constructed fiber laser is stable with an output power fluctuation relative to the average power of ∼ 3.24% (relative standard deviation) during the entire period.

The scanning spectrum over the FSR of the FFPI is presented in Fig. 5. A stable single-longitudinal-mode output was

achieved when the temperature of the laser cavity was controlled at 19.6 °C. Through the strict temperature control of the whole laser cavity, the laser operated stably in a single-frequency regime without mode hopping or mode competition as the pump power increased. Therefore, a 135 mW single-frequency DBR fiber laser operating at 1.95 μm was realized in a 2 cm long gain fiber when in-band pumped by a 1610 nm fiber laser.

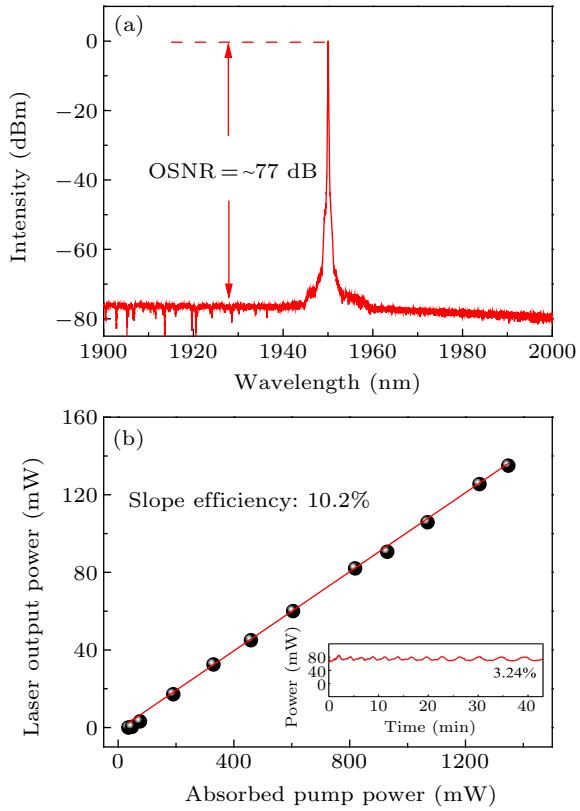


Fig. 4. (a) Measured output spectrum of the fiber laser. (b) The laser output power versus the absorbed pump power. The inset shows the power stability of the laser output power at 60 mW for 40 min.

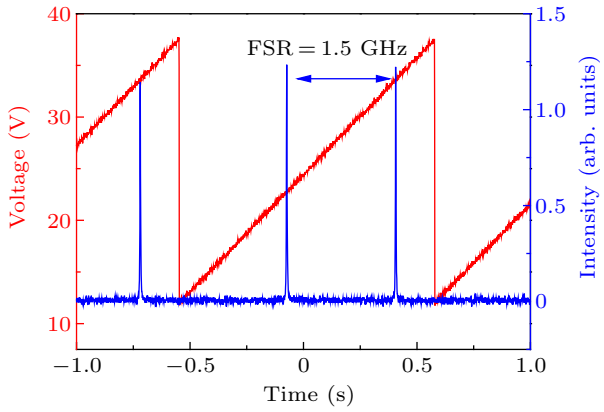


Fig. 5. The longitudinal modes characteristics of the single-frequency fiber laser measured by the scanning Fabry–Perot interferometer.

The laser linewidth was measured at a laser output power of 100 mW using the self-heterodyne method performed with a 3 km delay fiber (SMF-28M, Corning). Figure 6(a) shows the measured heterodyne signal which was fitted with a Lorentz lineshape. It can be observed that the signal is 90 kHz at 20 dB from the peak, indicating that the fiber laser has a linewidth of 4.5 kHz. Laser noise is an important parameter for a single-frequency fiber laser. Figure 6(b) shows the output RIN results under different laser output powers in the frequency range 0 MHz–15 MHz. The relaxation oscillation frequency peaks under different laser output powers were observed at frequencies of 0.55 MHz, 0.95 MHz, and 1.24 MHz, respectively. The relaxation oscillation frequency peaks move toward the higher frequency from 0.55 MHz to 1.24 MHz with increasing output power. The measured RIN is less than -140 dB·Hz^{-1} at frequencies above 10 MHz. Table 2 summarizes the performance of different single-frequency DBR fiber lasers based on RE ion-doped silica glass fiber and YAG-derived all-glass fibers. Here, the slope efficiency is defined as the slope of the curve obtained by plotting the laser output power versus the absorbed pump power. It can be found that the output power and the slope efficiency achieved in this work are higher than that in the single-frequency DBR Tm^{3+} doped silica fiber laser.[15] In addition, compared with the other single-frequency DBR YAG-derived all-glass fiber lasers, the performance of the 1.95 μm single-frequency DBR fiber laser achieved in this work is competitive. Further improvement should be made with respect to cavity design, such as optimizing the gain fiber numerical aperture (NA) and using high-NA FBGs to optimize the coupling efficiency of pump light.

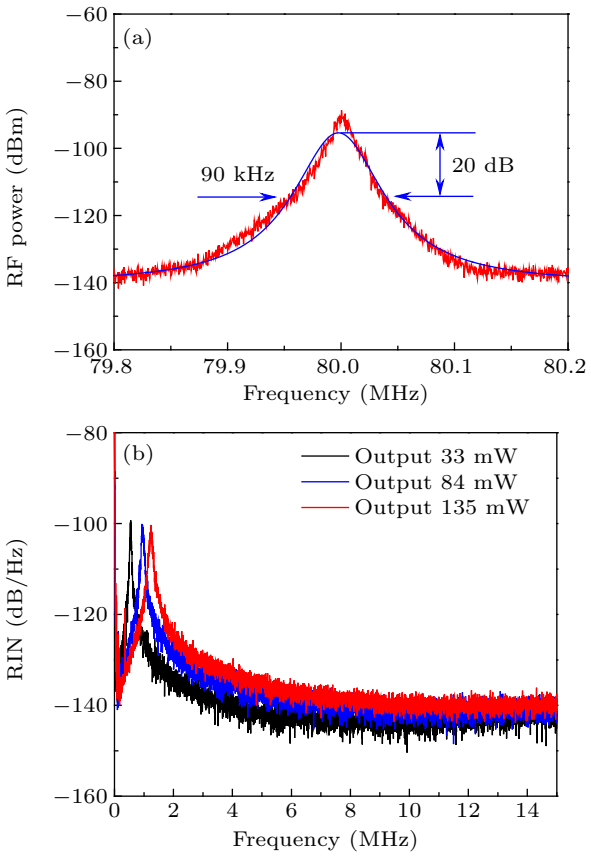


Fig. 6. (a) Linewidth of the single-frequency fiber laser measured by the self-heterodyne method. (b) RIN of the single-frequency fiber laser in the frequency band of 0 MHz–15 MHz with different output powers.

Table 2. Performance of different single-frequency DBR fiber lasers based on RE ion-doped silica fiber and YAG-derived all-glass fibers.

Precursor phase	Gain fiber length (cm)	Gain (dB/cm)	λ_{pump} (nm)	λ_{output} (nm)	Threshold (mW)	Output power (mW)	Slope efficiency (%)	Linewidth (kHz)	Reference
Tm:silica	1.8	–	1570	1920	250	50	9.1	36	[15]
Yb:YAG ceramic	1.7	3	976	1064	–	∼ 5	3.8	–	[19]
Er:YAG crystal	1.8	1.46	976	1550	–	24.2	15.1	–	[29]
Nd:YAG ceramic	1.8	1.57	808	1064	–	∼ 20	6	–	[30]
Tm:YAG ceramic	2	2.7	1610	1950	15.4	135	10.2	4.5	this work

4. Conclusion

In conclusion, a 1.95 μm single-frequency DBR fiber laser was realized by using a 2 cm long Tm:YAG ceramic-derived all-glass fiber pumped by a 1610 nm fiber laser. A maximum output power of 135 mW was obtained in this all-fiber integrated laser system with a linewidth of 4.5 kHz. The fiber laser has a high OSNR of ∼ 77 dB and a low pump threshold of ∼ 15.4 mW. In addition, the RIN was investigated under different laser output powers. These results indicate that high-gain Tm:YAG ceramic-derived all-glass fiber is a promising candidate in 2 μm single-frequency DBR fiber lasers.

Acknowledgments

Project supported by the Yunnan Fundamental Research Projects (Grant No. 202201AU070065), Natural Science Foundation of China for Young Scholars (Grant No. 52002131), Open Fund of the Guangdong Provincial Key Laboratory of Fiber Laser Materials and Applied Techniques (Grant No. 2021-04), and the Scientific Research Fund Project of Yunnan Provincial Department of Education (Grant No. 2022J0591).

References

[1] Wang W C, Zhou B, Xu S H, Yang Z M and Zhang Q Y 2019 *Prog. Mater. Sci.* **101** 90
[2] Wang C, Hao Q Q, Li W W, Huang H J, Wang S Z, Jiang D P, Liu J, Mei B C and Su L B 2020 *Chin. Phys. B* **29** 074205
[3] Zhang X, Yang F, Feng Z T, Zhao J J, Wei F, Cai H W and Qu R H 2019 *Chin. Phys. B* **28** 074209
[4] Liu J, Dong J F, Wang Y Y, Guo J, Xue Y Y, Xu J, Zhao Y G, Xu X D, Yu H H, Wang Z P, Xu X G, Chen W D and Petrov V 2021 *Opt. Lett.* **46** 4454
[5] He X, Xu S H, Li C, Yang C S, Yang Q, Mo S P, Chen D D and Yang Z M 2013 *Opt. Exp.* **21** 20800
[6] Zhang Z, Shen D Y, Boyland A J, Sahu J K, Clarkson W A and Ibsen M 2008 *Opt. Lett.* **33** 2059
[7] Fu S J, Shi W, Lin J C, Fang Q, Sheng Q, Zhang H W, Wen J W and Yao J Q 2015 *Opt. Lett.* **40** 5283
[8] Walasik W, Traoré D, Amavigan A, Tench R E, Delavaux J M and Pinsard E 2021 *J. Lightwave Technol.* **39** 5096
[9] Fu S J, Shi W, Feng Y, Zhang L, Yang Z M, Xu S H, Zhu X S, Norwood R A and Peyghambarian N 2017 *J. Opt. Soc. Am. B* **34** A49
[10] Wang Q, Geng J H, Luo T and Jiang S B 2009 *Opt. Lett.* **34** 3616
[11] Tang G W, Zhang Y T, Yang D L, Lin W, Huang W H, Tu L, Wu F, Yan N, Qian Q, Wei X M and Yang Z M 2021 *Opt. Lett.* **46** 2027
[12] Geng J H, Wang Q, Luo T, Jiang S B and Amzajerdian F 2009 *Opt. Lett.* **34** 3493
[13] Tang G W, Wen X, Huang K M, Qian G Q, Lin W, Cheng H H, Jiang L C, Qian Q and Yang Z M 2018 *Appl. Phys. Exp.* **11** 032701
[14] Qian G Q, Wang W L, Tang G W, Guan X C, Lin W, Qian Q, Chen D D, Yang C S, Liu J T, Zhou G Y, Xu S H and Yang Z M 2020 *Opt. Lett.* **45** 1047
[15] Fu S J, Shi W, Sheng Q, Shi G N, Zhang H W, Bai X L and Yao J Q 2017 *IEEE Photonic. Tech. Lett.* **29** 853
[16] Wen X, Tang G W, Wang J W, Chen X D, Qian Q and Yang Z M 2015 *Opt. Exp.* **23** 7722
[17] Geng J H, Wu J F, Jiang S B and Yu J R 2007 *Opt. Lett.* **32** 355
[18] Hofmann P, Voigtlander C, Nolte S, Peyghambarian N and Schulzgen A 2013 *J. Lightwave Technol.* **31** 756
[19] Zhang Y M, Wang W W, Li J, Xiao X S, Ma Z J, Guo H T, Dong G P, Xu S H and Qiu J R 2019 *J. Am. Ceram. Soc.* **102** 2551
[20] Liu Z J, Xie Y Y, Cong Z H, Zhao Z G, Jia Z X, Li C Z, Qin G S, Wang S, Gao X B, Shao X B and Zhang X Y 2019 *Opt. Lett.* **44** 4307
[21] Xie Y Y, Liu Z J, Cong Z H, Qin Z G, Wang S, Jia Z X, Li C Z, Qin G S, Gao X B and Zhang X Y 2019 *Opt. Exp.* **27** 3791
[22] Tang G W, Qian G Q, Lin W, Wang W L, Shi Z G, Yang Y, Dai N L, Qian Q and Yang Z M 2019 *Opt. Lett.* **44** 3290
[23] Ballato J, Hawkins T, Foy P, Kokuoz B, Stolen R, McMillen C, Daw M, Su Z, Tritt T M, Dubinskii M, Zhang J, Sanamyan T and Matthewson M J 2009 *J. Appl. Phys.* **105** 53110
[24] Zhang Y M, Qian G Q, Xiao X S, Tian X L, Ding X Q, Ma Z J, Yang L Y, Guo H T, Xu S H, Yang Z M and Qiu J R 2018 *J. Am. Ceram. Soc.* **101** 4627
[25] Dragic P, Law P C, Ballato J, Hawkins T and Foy P 2010 *Opt. Exp.* **18** 10055
[26] Dragic P, Hawkins T, Foy P, Morris S and Ballato J 2012 *Nat. Photon.* **6** 627
[27] Zhang Y M, Qian G Q, Xiao X S, Tian X L, Chen Z, Zhong J P, Ma Z J, Guo H T, Xu S H, Yang Z M and Qiu J R 2018 *J. Am. Ceram. Soc.* **101** 1616
[28] Zheng S P, Li J, Yu C L, Zhou Q L and Chen D P 2016 *Opt. Exp.* **24** 24248
[29] Xie Y Y, Cong Z H, Zhao Z G, Zhang X Y, Zhao X, Zhao W, Shao X B and Liu Z J 2021 *J. Lightwave Technol.* **39** 4769
[30] Zhang Y M and Qiu J R 2018 *Proceedings of the Asia Communications and Photonics Conference* p. 8595750